Title

Cardiac Electrophysiological Substrate Underlying the ECG Phenotype and Electrogram Abnormalities in Brugada Syndrome Patients

Journal

Circulation, 131(22)

ISSN

0009-7322

Authors

Zhang, Junjie
Sacher, Frédéric
Hoffmayer, Kurt
et al.

Publication Date

2015-06-02

DOI

10.1161/circulationaha.114.013698

Peer reviewed

Published in final edited form as:

Circulation. 2015 June 2; 131(22): 1950–1959. doi:10.1161/CIRCULATIONAHA.114.013698.

The Cardiac Electrophysiologic Substrate Underlying the ECG Phenotype and Electrogram Abnormalities in Brugada Syndrome Patients

Junjie Zhang, BS[1,2], **Frédéric Sacher, MD**[3], **Kurt Hoffmayer, MD**[4], **Thomas O'Hara, PhD**[5], **Maria Strom, PhD**[6], **Phillip Cuculich, MD**[1,7], **Jennifer Silva, MD**[1,7], **Daniel Cooper, MD**[1,7], **Mitchell Faddis, MD**[1,7], **Mélèze Hocini, MD**[3], **Michel Haïssaguerre, MD**[3], **Melvin Scheinman, MD**[8], and **Yoram Rudy, PhD**[1,2,7]

[1]Cardiac Bioelectricity and Arrhythmia Center, Washington University, St. Louis, MO

[2]Department of Biomedical Engineering, Washington University, St. Louis, MO

[3]Bordeaux University Hospital, LIRYC institute, Pessac, France

[4]School of Medicine, University of Wisconsin, Madison, WI

[5]Institute for Computational Medicine, Johns Hopkins University, Baltimore, MD

[6]CardioInsight Technologies, Cleveland, OH

[7]School of Medicine, Washington University, St. Louis, MO

[8]School of Medicine, The University of California, San Francisco, CA

Abstract

Background—Brugada syndrome (BrS) is a highly arrhythmogenic cardiac disorder, associated with an increased incidence of sudden death. Its arrhythmogenic substrate in the intact human heart remains ill-defined.

Methods and Results—Using noninvasive ECG imaging (ECGI), we studied 25 BrS patients to characterize the electrophysiologic substrate, and 6 patients with right bundle branch block (RBBB) for comparison. Seven normal subjects provided control data. Abnormal substrate was observed exclusively in the right ventricular outflow tract (RVOT) with the following properties (compared to normal controls; $p<0.005$): (1)ST-segment elevation (STE) and inverted T-wave of

Correspondence: Yoram Rudy, PhD, Director, Cardiac Bioelectricity and Arrhythmia Center, Campus Box 1097, One Brookings Drive, Washington University in St. Louis, St. Louis, MO 63130, Phone: 314-935-8160, Fax: 314-935-8168, rudy@wustl.edu.

Disclosures: Dr. Sacher received consultant fees and speaker honoraria from Biosense Webster, St. Jude Medical, Sorin Group, Medtronic and Biotronik. Dr. Strom is a paid employee and stockholder of CardioInsight Technologies. Dr. Cuculich received research support from National Institutes of Health and March of Dimes. Dr. Silva received consultant fees and speaker honoraria from Medtronic, AliveCor. Dr. Faddis received research support from Stereotaxis. Dr. Cooper received consultant fees and speaker honoraria from Boston Scientific, St. Jude Medical, Medtronic, and Biotronik. Dr. Hocini received lecture fees from Medtronic and St. Jude Medical, served on the advisory board for Medtronic and is a stockholder of CardioInsight Technologies. Dr. Haïssaguerre is a stockholder of CardioInsight Technologies and received lecture fees from Biosense Webster and Medtronic. Dr. Scheinman received consultant fees and speaker honoraria from St. Jude Medical, Medtronics, Boston Scientific and Biotronik. Dr. Rudy cochairs the scientific advisory board, holds equity in and receives royalties from CardioInsight Technologies. CardioInsight Technologies does not support any research conducted in Dr. Rudy's laboratory. All other authors have reported that they have no relevant relationships to disclose.

unipolar electrograms (EGMs) (2.21±0.67 vs. 0 mV); (2)delayed RVOT activation (82±18 vs. 37±11 ms); (3)low amplitude (0.47±0.16 vs. 3.74±1.60 mV) and fractionated EGMs, suggesting slow discontinuous conduction; (4)prolonged recovery time (RT; 381±30 vs. 311±34 ms) and activation-recovery intervals (ARIs; 318±32 vs. 241±27 ms), indicating delayed repolarization; (5)steep repolarization gradients (ΔRT/Δx= 96±28 vs. 7±6 ms/cm, ΔARI/Δx= 105±24 vs. 7±5 ms/cm) at RVOT borders. With increased heart rate in 6 BrS patients, reduced STE and increased fractionation were observed. Unlike BrS, RBBB had delayed activation in the entire RV, without STE, fractionation, or repolarization abnormalities on EGMs.

Conclusions—The results indicate that both, slow discontinuous conduction and steep dispersion of repolarization are present in the RVOT of BrS patients. ECGI could differentiate between BrS and RBBB.

Keywords

Brugada Syndrome; Electrophysiology; Electrocardiographic imaging (ECGI)

Introduction

Brugada syndrome (BrS) is an inherited disorder, affecting predominantly males in their 40s[1] and associated with an increased incidence of sudden cardiac death (SCD). It presents with ECG expression of atypical right bundle branch block (RBBB) pattern and ST-segment elevation (STE) in leads V1–V3.[1–2] It is estimated that BrS causes approximately 20% of SCD in cardiac patients with structurally normal hearts.[1] Understanding its pathophysiological mechanisms is essential for improving risk stratification, diagnosis and treatment to prevent SCD.

BrS is considered a primary electrical cardiac disease, since no structural anomalies are detected by conventional imaging. Up to 30% of patients test positive for mutations in the SCN5A gene,[1] which causes a loss-of-function of the cardiac sodium channel (I_{Na}). A Brugada ECG pattern can be provoked, in some affected patients with a normal baseline ECG pattern, by administration of I_{Na} blockers.

There are two leading hypotheses for mechanisms underlying BrS phenotype and arrhythmias. (1) *The abnormal repolarization hypothesis (based on the canine wedge preparation)*:[3–5] Phase-1 notch is present in epicardial action potentials (AP) due to a high density of transient outward current (I_{to}), but absent in endocardial APs (low I_{to} density). A reduced I_{Na} in BrS exaggerates the phase-1 notch preferentially in right ventricular outflow tract (RVOT) epicardium, where I_{to} is expressed with maximal density. The resulting voltage gradients give rise to STE on the ECG. Further outward shift of the balance between I_{Na} and I_{to} can repolarize the membrane during phase-1 below the voltage range for L-type calcium channels ($I_{Ca\text{-}L}$) activation. When $I_{Ca\text{-}L}$ fails to activate, the AP loses its plateau (dome). Spatially heterogeneous loss of the AP plateau in the RVOT can lead to reentry (termed “phase-2 reentry” by Antzelevitch and colleagues). (2) *The abnormal conduction hypothesis (based on whole–heart studies in BrS patients)*:[6–8] Impaired I_{Na} in structurally deranged tissue causes slow discontinuous AP propagation. Asynchronous activation can promote reentrant arrhythmias and create voltage gradients, causing STE and fractionation

on the ECG. Data from catheter mapping[6] showed that delayed conduction and abnormal electrograms (EGMs) with low voltage and fractionated late potentials (reflecting slow discontinuous conduction) were exclusively localized in the anterior aspect of the RVOT epicardium. Catheter ablation in this area normalized the Brugada ECG and prevented ventricular tachycardia (VT). The pathophysiological mechanisms of the abnormal ECG and arrhythmia in BrS are still a subject of debate.

While much is known at the molecular and cellular scales, understanding the cause of the BrS ECG pattern and associated arrhythmias requires detailed characterization of the electrophysiologic (EP) substrate in the intact hearts of BrS patients. This requires high resolution, panoramic EP mapping of the ventricles and cannot be achieved with invasive catheter mapping. The recent development of noninvasive mapping with Electrocardiographic Imaging (ECGI) allowed us to obtain the first high resolution panoramic EP data from BrS patients, including up to 1500 unipolar epicardial EGMs and epicardial maps of activation and repolarization.[9–15] Based on these data recorded during sinus rhythm (SR), we characterized the EP substrate in BrS patients in an effort to provide insight into the mechanistic origin of the BrS phenotype. The results show that both, repolarization and structurally-based conduction abnormalities coexist in hearts of BrS patients. We also compared the BrS EP substrate to non-BrS RBBB (generally considered benign) to determine whether the substrate is specific to BrS, and whether ECGI can differentiate between these two pathologies with similar ECGs.

Methods

Patient Population

Twenty-five BrS patients from two centers in the United States and one in France were enrolled. Details on patient recruitment are provided in Supplemental Methods. The BrS diagnosis was based on the consensus criteria[1] and was the basis for patient recruitment. Beyond the consensus criteria, pregnant women and children were excluded. Patient demographic data are provided in Supplemental Table 1. Six RBBB patients with a prolonged QRS>120ms were studied for comparison. All BrS and RBBB patients had no evidence of structural heart disease on echocardiography or MRI. Data from seven normal subjects[12] provided normal control. Subject characteristics are provided in Supplemental Table 2. Protocols were approved by the Institutional Review Boards at the three centers; written informed consent was obtained from all patients.

Noninvasive Mapping

ECGI methodology was described previously[9–14] (Supplemental Figure 1A). Briefly, torso surface ECG potentials, recorded simultaneously from 250 electrodes, were combined mathematically with patient-specific heart-torso geometry from ECG-gated computed tomography (CT) to construct epicardial potentials, unipolar EGMs, and maps of epicardial activation and repolarization. Bipolar EGMs were constructed for fractionation analysis. The method was validated extensively for reconstruction of EGMs,[9–10] activation[11–12] and repolarization.[10, 12] Additional validation references are provided in Supplemental References. Spatial properties of the EP substrate were determined by dividing the

epicardium into 6 segments based on CT images (Supplemental Table 3; the RVOT is depicted in Supplemental Figure 1B). EGMs from valvular regions were excluded. On average, 1154 EGMs/patient were used for analysis.

EGMs were evaluated for morphology, magnitude and fractionation. EGM Brugada morphology was defined as STE followed by T-wave inversion. EGM magnitude (EMM) was measured peak-to-peak during the EGM QRS; for fractionated EGMs, the measurement was confined to the fractionated segment. Fractionation was expressed as number of low-amplitude deflections per EGM and displayed on epicardial EGM deflection maps (EDMs).[13] For the fractionation analysis, bipolar EGMs were approximated by time derivatives of unipolar EGMs.

Local activation time (AT, referenced to beginning of QRS in ECG lead II) was determined by the maximal negative slope of the EGM during QRS inscription (Supplemental Figure 1C). From the ATs, epicardial activation isochrone maps were created. Slow conduction is represented by crowded isochrones. Regional activation duration (AD) was defined as the interval between the earliest and latest AT in a region, considering all EGMs in that region.

Local recovery time (RT) was determined from the maximal positive slope of the EGM T-wave (Supplemental Figure 1C); it reflects the sum of local activation time and local action potential duration (APD). For a given activation sequence, RT determines spatial voltage gradients during repolarization, and underlies ST-T deflections. RT dispersion provides substrate for unidirectional block and reentry. Activation-recovery interval (ARI) was defined as the difference between RT and AT. ARI is independent of AT and a surrogate for local APD.[16] Epicardial RT and ARI gradients were computed as the difference between neighboring epicardial nodes, divided by the distance between them.

ECGI was conducted in 6 patients during increased heart rate (HR; 3 with exercise and 3 with isoprenaline). ECGI maps at baseline and during the faster HR were compared.

Simulation

The O'Hara-Rudy (ORd) model of a human ventricular myocyte[17] was used in the simulations. Fast/late I_{Na} and I_{to} were replaced by formulations used previously to represent the prominent phase-1 repolarization notch characteristic of RVOT APs.[18] The model was paced to steady state at normal and slow rates (1,000 beats at 1 and 0.5 Hz, respectively) with various combinations of reduced I_{Na} and enhanced I_{to} conductances (G_{Na} and G_{to}). Combinations were selected to span a virtual Brugada severity space. APD was measured at 90% repolarization (APD90 in ms).

Statistical Analysis

For every subject, the mean values for EGM variables within each epicardial segment were computed. All statistical tests were performed at the level of epicardial segments. Differences in variables among epicardial segments were compared by one-way repeated measures ANOVA. When the assumption of sphericity was violated, Greenhouse-Geisser correction was performed. Using the Bonferroni method, pairwise comparisons between RVOT and other regions were conducted (5 tests in total). Continuous variables at baseline

and increased HR were compared by paired t-test. Continuous variables between BrS and control, and between BrS and RBBB were compared by unpaired t-test. The Satterthwaite modified t-test was used for variables with unequal variances. All tests with $P<0.05$ were considered statistically significant. Statistical analysis was performed using SPSS v19.

Results

BrS Abnormal EGM Characteristics and Localization

Table 1A summarizes values of EGM parameters in each epicardial segment for baseline HR. Pairwise multiple comparisons between the RVOT and other regions suggest that the abnormal substrate is localized in the RVOT. Figure 1 shows EGM characteristics and localization for representative examples in 3 BrS patients (normal maps are provided for reference). STE (examples in Panel A) was observed in RVOT of all 25 patients (2.21±0.67 vs. 0 mV in control, $p<0.005$), but rarely detected outside the RVOT. Three patients had low-magnitude STE in the RV free wall and two in the left ventricular (LV) free wall (range from 0.2 to 0.5 mV). ECG leads with STE for all patients are identified in Supplemental Table 1. 59% of EGMs in RVOT had STE>1 mV. EGMs magnitude (Panel B) was lower in the RVOT (0.47±0.16 vs. 3.74±1.60 mV in control, $p<0.005$) than in other regions (>2.5mV). 46% of EGMs in the RVOT had voltage<2 mV. Four patients had low voltage in the RV free wall and 3 in the LV base. Fractionated EGMs (Panel C) were present in the RVOT (number of deflections =2.97±0.69 vs. 0 in control, $p<0.005$). 27% of EGMs in the RVOT had more than 2 deflections. Two patients had fractionated EGMs in the RV free wall. Panel D shows EGMs from locations marked by white dots in Panel C, representative of abnormal morphology of RVOT EGMs. Red arrows indicate low voltage and fractionated EGMs.

BrS Activation

Normal human epicardial activation patterns during SR were reported previously.[12, 19] In general, earliest epicardial activation occurs in anterior RV (although there are many variants of location),[12, 19] while lateral LV base is most commonly the latest region to activate. Activation isochrone maps in Figure 2A show examples of how SR epicardial activation patterns were altered by the presence of BrS EP substrate. Patient BrS#4 had earliest epicardial breakthrough (asterisk) over the RV free wall, from which activation propagated slowly (crowded isochrones) across the RVOT-RV free wall border. RV free wall and LV activated first, leaving the anterior RVOT to activate last (light blue). Patient BrS#15 had a similar activation pattern, with a broader wavefront and faster activation of the RV free wall. Slow conduction occurred in the RVOT (crowded isochrones in the blue region). Patient BrS#20 had earliest activation in the anterior RV. Latest activation (dark blue) occurred at the lateral RVOT, nearly 65 ms after the anterior RV breakthrough.

Of the 25 BrS patients imaged during SR, 20 demonstrated altered or delayed epicardial activation at the RVOT. Table 1B summarizes AT (mean ± standard deviation) in each segment. AT in RVOT (82±18 vs. 37±11 ms in control, $p<0.005$) was almost as late as that of LV base (80±16 ms), and was much delayed compared to the other 4 segments. In specific RVOT locations, AT was as late as 150 ms. AD (the time needed for activation of a

defined region) was calculated for the RVOT (36±16 ms), the RV free wall (16±3 ms), the entire RV (40±14 ms), the entire LV (27±5 ms) and both ventricles (51±10 ms). RVOT activation took much longer than RV free wall or LV. AD of the RVOT accounted for about 71% of total AD in both ventricles, highlighting the slow activation of the RVOT.

BrS Repolarization

Figure 2B–C shows representative ARI and RT maps from 3 BrS patients. Table 1B provides ARI and RT in each epicardial segment. ARI prolongation (318±32 vs. 241±27 ms in control, $p<0.005$) and RT prolongation (381±30 vs. 311±34 ms in control, $p<0.005$) were observed primarily in the RVOT, but also extended into adjacent neighboring regions of the RV free wall and the LV free wall. Steep epicardial ARI gradients and RT gradients (red arrows) occurred mostly at the RVOT-RV free wall or RVOT-LV free wall borders. These gradients also existed within the RVOT. Transitions of colors from blue to red across these regions reflect large differences in ARI and RT of 70–140 ms, leading to very steep localized ARI gradients (105±24 vs. 7±5 ms/cm in control[12], $p<0.005$) and RT gradients (96±28 vs. 7±6 ms/cm in control, $p<0.005$). In patient BrS#15, the gradients between the anterior and lateral RVOT ARI map are not apparent in the RT map. This is because the anterior RVOT activated about 40 ms later than the lateral RVOT. This long delay masks the ARI differences between these two regions. However, in regions that activate without conduction delay (e.g., RV free wall) RTs and their dispersion are primarily determined by ARI and ARI dispersion, independent of conduction. The patterns in RT maps closely follow the ARI patterns in such cases.

Effects of Increased HR in BrS

ECGI was performed in 6 BrS patients during increased HR (mean increase from 71 to 133 BPM) Figure 3 shows the effects of increased HR (from 72 to 115 BPM) in one representative example. Although the activation sequence remained largely unchanged (Panel A), RVOT activation was further delayed with HR increase (AD: from 32±7 ms to 38±10 ms), and RVOT EGMs had more fractionation and lower voltage (Panels D–F). This change of RVOT EGMs was observed in 4 out of 6 patients (no significant change in the other 2 patients). When HR increased, ARIs (Panel B, corrected for HR) were shorter over the entire heart, but the RVOT ARIs decreased more than in other regions (by 50 ms compared to 25 ms in RV free wall). The regions with steep ARI gradients persisted, but the magnitude of the ARI gradient decreased (from 117 ms/cm to 96 ms/cm). Reductions in RT and RT gradients were also observed during increased HR. STE (Panel C) in RVOT was significantly reduced (from 2.0 mV to 0.5 mV). Similar changes in ARI, RT and STE were observed in all 6 patients (Table 1C).

Comparison between BrS and Non-BrS RBBB

ECGI was conducted during sinus rhythm in 6 non-BrS patients with RBBB, without structural heart disease. Epicardial activation patterns, ARI maps and EGM morphologies were analyzed and compared to those of the BrS patients. This comparison is of clinical importance, because the diagnosis of BrS in the presence of an RBBB ECG could be challenging. This is demonstrated in Figure 4A, where the Brugada ECG pattern for BrS#10 is masked by an RBBB pattern. Figure 4 shows representative data from 4 patients (2 BrS

and 2 RBBB). BrS#4 had a spontaneous Brugada ECG pattern, while the ECG of BrS#10 showed an atypical RBBB pattern. Supplemental Table 4 summarizes the differences of ECGI parameters between all BrS and RBBB patients. In RBBB patients, activation of the entire RV was delayed, with a long conduction delay of 35 ms across the interventricular septum (crowded isochrones; black arrow). In contrast, delayed activation was confined to the RVOT of BrS patients. Normal RV epicardial breakthrough (indicative of normal conduction system participation) was observed in all BrS patients, but not in any RBBB patient. BrS patients had a much longer AD in the RVOT than RBBB patients (36±16 ms BrS vs. 14±5 ms RBBB; $p<0.005$), accounting for most of the AD in the entire RV (40±14 ms BrS vs. 24±6 ms RBBB; $p<0.005$). Unlike BrS, RBBB T-wave inversion in the RVOT and RV was not accompanied by ARI prolongation (RBBB=246±25 ms, BrS=326±30 ms, $p<0.005$), steep ARI dispersion (RBBB=8±4 ms/cm, BrS=105±24 ms/cm, $p<0.005$) or steep RT gradients (RBBB=6±3 ms/cm, BrS=96±28 ms/cm, $p<0.005$); ARI and RT maps were uniform. This demonstrates that T-wave inversion *per-se* does not indicate the presence of repolarization gradients. The abnormal EGM characteristics specific for BrS (STE and low amplitude fractionation) were not observed in RBBB patients. It is of note that ECGI unmasked the presence of BrS in BrS#10, who had an RBBB pattern on the body surface ECG but BrS substrate in the RVOT, as revealed by ECGI.

Discussion

This is the first panoramic ventricular mapping study in BrS patients, made possible by ECGI. The panoramic mapping identified the RVOT as the region of abnormal EP substrate with the following properties: (1)Abnormal EGMs characterized by STE and inverted T-wave, reduced amplitude and fractionation; (2)Conduction delays and regions of slow conduction; (3)Prolonged repolarization and steep repolarization gradients; (4)Reduced STE, increased fractionation, decreased RVOT ARI and RT, decreased ARI and RT gradients with increased HR. These properties are significantly different than in patients with RBBB.

Abnormal EGM Characteristics and Localization

The RVOT has been suggested as the origin of arrhythmic activity in BrS patients.[1, 6, 8, 20–21] Our observation of substrate localization exclusively to the RVOT in BrS patients provides crucial evidence for the RVOT dominant role in clinical BrS. This is in contrast to a recent ECGI study of the long QT syndrome, where abnormal repolarization substrate was spread over the entire epicardium.[15] ECGI revealed RVOT EGMs with coved morphology similar to the typical Brugada ECG morphology in the body surface right precordial leads (Figure 1). Additionally, the EGMs were of low amplitude and fractionated. These EGM properties, reconstructed noninvasively by ECGI, were consistent with those obtained from invasive electroanatomical mapping.[6, 20] The ECGI panoramic mapping determined that the majority of these Brugada EGMs were confined to the RVOT; only rarely were they detected close to the RVOT, in adjacent neighboring regions of the RV or LV free wall. Therefore, our study adds insight to the observation from invasive epicardial mapping and ablation, that the Brugada morphology normalized following ablation in the

anterior RVOT.[6] This EGMs localization confirms that the RVOT is the origin of the Brugada-type ECG morphology in the body surface right precordial leads.

Substrate for Abnormal Conduction

BrS has been considered a primary electrical disease, because structural abnormalities have not been detectable by noninvasive clinical imaging (e.g. echocardiography or MRI). Recently, RV interstitial derangements (fibrosis, fatty infiltration) have been found in endomyocardial biopsies of BrS patients,[7] as well as in the explanted heart of a BrS patient carrying an SCN5A mutation.[22] Fibrosis and fatty infiltration have been associated with decreased electric coupling, discontinuous propagation and reduced conduction velocity.[23] In the normal heart, excitability and conduction are dominated by I_{Na}. In BrS, where I_{Na} is impaired, I_{to} becomes a significant determinant of excitability, opposing the depolarizing effect of I_{Na}. This is especially true in the RVOT, where I_{to} is expressed with very high density. In this region, the balance between reduced depolarizing I_{Na} and large repolarizing I_{to} results in a reduced excitatory current, which on the background of a structurally abnormal substrate, can support long localized conduction delays and discontinuous slow conduction, conditions that facilitate sustained reentrant arrhythmias.[23]

Experimental, theoretical, and clinical studies have shown that low-magnitude, fractionated and wide EGMs reflect slow, non-uniform and discontinuous conduction through a structurally heterogeneous substrate associated with separation and reduced coupling of myocardial fibers.[24] Previous studies demonstrated ECGI's ability to reconstruct EGMs with these properties.[9, 13–14] In this study, ECGI reconstructed low-magnitude, fractionated and wide unipolar EGMs. The time derivatives (dV/dt) of unipolar EGMs approximate bipolar EGMs and emphasize fractionation (Figure 1D, red). The reconstructed unipolar EGMs and the approximated bipolar EGMs are consistent with those measured directly by catheters in BrS patients,[6, 20] providing evidence for slow discontinuous conduction in the RVOT. The ECGI mapping of late RVOT activation, prolonged AD, presence of regions of slow conduction, and altered wavefront propagation compared to normal (Figure 2A) provides additional evidence supporting the conduction hypothesis. Similar observations were made with invasive mapping.[6, 20] Computer modeling of AP conduction in presence of BrS mutant I_{Na} also produced slow discontinuous conduction, causing spatial gradients of membrane potential during the AP plateau and/or early repolarization phase and STE in the computed pseude-ECG waveform.[25] Taken together, these data provide evidence for the presence of abnormal conduction in the RVOT of BrS patients.

Antzelevitch and collegues used a canine RV wedge preparation, where I_{to} activator and sodium and calcium channel blockers were applied to pharmacologically simulate effects of BrS, and to explain EGM fractionation and late potentials.[3–4] This preparation did not include structural abnormalities and conduction disturbances; it investigated the mechanism of EGM fractionation in the setting of abnormal repolarization alone. It demonstrated the ability to generate secondary deflections on the epicardial EGMs based on differences in the AP morphology at different epicardial locations during the AP repolarization phase. Following the phase-1 notch (which underlies the STE), APs can differ by the presence/amplitude of a dome and by the time of complete repolarization. The associated gradients

can result in 2 late deflections on the EGM.[4] Because the deflections occur during late repolarization, the shortest coupling interval to the main EGM deflection (generated by the AP upstroke) was 200 ms.[4]

In the patients studied here, and in patients studied using catheters,[6] EGM fractionation shows different properties; it includes more than 2 deflections (many show 4 deflections) that are tightly coupled to the main deflection (<50 ms) and even occur before the main deflection. Moreover, the fractionation is amplified with increased heart rate. All of these properties point to fragmented slow conduction as a major contributor to EGM fractionation. Of course, abnormal repolarization can also contribute to fractionation of the EGM,[4] but the augmentation with increased heart rate identifies conduction as the major mechanism.

Substrate for Abnormal Repolarization

I_{to} expression is non-uniform in the ventricular myocardium. Expression is highest in the epicardium and diminishes transmurally towards the endocardium, creating a phase-1 notch in epicardial, but not endocardial AP. A particularly large I_{to} density is found in the epicardial RVOT. Reduced I_{Na} in BrS on the background of the large I_{to} exaggerates the phase-1 notch, and the resulting spatial gradients of membrane voltage can give rise to STE in ECG waveforms. The deep and wide notch delays the AP plateau and prolongs APD, potentially causing reversal of membrane voltage gradients and T wave inversion.[3, 5] In extreme cases (not recorded in this study), the membrane is repolarized to voltages that are too low for sufficient $I_{Ca\text{-}L}$ activation during phase-1 of the AP and cells repolarize prematurely, losing the AP plateau.[3] This bi-phasic behavior (APD prolongation followed by APD shortening in conditions of extreme severity) is supported by the computer simulations of Figure 5. ECGI was validated to accurately map regions of altered repolarization and steep repolarization gradients.[10] The ECGI mapping in this study (Figure 2) demonstrated delayed repolarization and prolonged epicardial APDs (based on reconstructed ARIs) in the RVOT of BrS patients. Short ARIs, closely coupled extrasystoles, or VT were not recorded in any patient. Interestingly, direct recordings from endocardium and epicardium revealed longer ARIs in epicardium than in endocardium of BrS patients, suggesting prolongation of epicardial APD; ARI shortening was not reported.[26] A steep repolarization gradient existed at the RVOT borders, which could be due to non-uniform spatial expression of the mutation. However, even uniform spatial distribution of mutant-channel current can cause spatial ARI dispersion. APD is determined by a delicate balance of transmembrane currents and this dependence is non-linear. Therefore, spatially uniform mutant I_{Na} expression on the background of non-uniform electrophysiologic profile (heterogeneous I_{to}) can cause large spatial variation of the APD. It is also possible that reduced coupling and fiber separation in the BrS substrate limit electrical loading and help maintain the steep spatial repolarization gradients.

Examining the Coexistence of Conduction and Repolarization Substrates Using Increased HR

The rate-dependence of STE and EGM fractionation in BrS may be helpful in unmasking the existence of abnormal repolarization and abnormal conduction, respectively, in the EP substrate. Decreased STE at increased HR supports the repolarization hypothesis, because it

suppresses the AP phase-1 notch and associated voltage gradients. In this study, STE in the RVOT decreased in all 6 patients with increased HR. In contrast, increased EGM fractionation with increased HR reflects the presence of slow discontinuous conduction, consistent with the conduction hypothesis. Increased RVOT EGM fractionation was observed in 4 patients at faster HR. Taken together, the effects of increased HR on STE and EGM fractionation support coexistence of these two mechanisms in the BrS substrate. Repolarization abnormality is the major contributor to STE, while conduction abnormality is the major contributor to EGM fractionation.

From the arrhythmogenic perspective, the presence of steep repolarization gradients (dispersion) introduces asymmetry of excitability and thus conditions for unidirectional block.[23] Slow conduction shortens the wavelength of the reentrant AP, thus allowing for shorter reentry pathways and stabilizing reentry. Together, these two properties provide conditions for sustained reentrant excitation. Their coexistence in the substrate of BrS patients has been suggested by other recent studies;[27–28] it is consistent with the high incidence of arrhythmic SCD. Interestingly, most arrhythmic events occur during bradycardia. Reduced STE at increased HR reflects less steep repolarization gradients; it reduces arrhythmogenicity because the probability for unidirectional block is reduced.

Comparison to Non-BrS RBBB

BrS and RBBB differ greatly in their arrhythmogenicity, with BrS being highly arrhythmogenic. Therefore, a noninvasive method for distinguishing between these abnormalities is highly desirable. Despite the similarities in the 12-lead ECG, ECGI differentiated BrS from non-BrS RBBB in several aspects: (1)BrS EGMs with STE, low voltage and fractionation were not found in RBBB. (2)Non-delayed RV epicardial breakthrough was observed in all BrS patients, indicating involvement of a functioning RBB. RV breakthrough was absent in all RBBB patients, reflecting the defective conduction system. (3)In BrS, slow discontinuous conduction and delayed activation were confined to the RVOT and RVOT-RV border. In contrast, RBBB caused late activation of the entire RV because of a long conduction delay across the septum; there were no regional conduction delays within the RVOT/RV. (4)ARI prolongation and steep ARI gradients were observed in RVOT of BrS patients but not in RBBB patients. These differences could provide the basis for an ECGI-based differential diagnosis in the clinical setting. In addition, the BrS ECG pattern may be masked by an RBBB ECG pattern in some patients, causing difficulties in distinguishing between BrS and RBBB. This has led to invasive procedures (e.g., RV pacing in Chiale intervention[29]) that help unmask the Brugada phenotype in patients with RBBB. In this study, we demonstrated that ECGI can image the BrS substrate in such patients, providing a noninvasive method for the clinical diagnosis of BrS even when it is masked by an RBBB pattern on the body surface ECG.

Conclusions

Noninvasive ECGI reveals that the abnormal EP substrate in BrS patients is localized in the RVOT. Both abnormal repolarization and abnormal conduction are present in the substrate, leading to steep repolarization gradients and delayed activation. In addition, ECGI could

differentiate BrS from RBBB based on differences in patterns of activation and repolarization, and electrogram morphology.

Limitations

Being the first ECGI study of BrS patients, it does not differentiate between subgroups (genotype, symptoms, family history etc.) within the BrS population.

ECGI data for the normal controls were previously obtained with the same ECGI methodology; the data were not obtained at the time of this study.

This study is limited to characterizing the BrS substrate from data obtained during SR, and relating its properties to the BrS ECG and EGM phenotype. Results demonstrate the existence of substrate with steep dispersion of repolarization and slow conduction, conditions that facilitate reentrant arrhythmias. However, arrhythmias were not recorded in any of the patients and the study does not provide direct information about the mechanism of VT in BrS patients. Typically, BrS I_{Na} is reduced to approximately 50% relative to control. Figure 5 shows simulated behavior for a large range of I_{Na} reduction, paired with a range of I_{to} to account for its high density in the RVOT. Deepening and broadening of the phase-1 notch, resulting in APD prolongation, is obtained for the entire range of I_{Na} with G_{to}>=1.5 times control. The accentuated notch and resulting transmembrane voltage gradients contribute to STE in BrS EGMs. However, loss of the dome and APD shortening at 50% I_{Na} required Gto>=3.3 times control (at 1 Hz pacing). A previously characterized BrS gain-of-function mutation in I_{to}, L450F, was associated with a similarly large degree (~3-fold) of current increase.[30] It should be mentioned that the simulations were conducted in an isolated cell. In the multicellular substrate of BrS hearts, electrical loading on the AP dome during localized conduction delays (due to structural derangement) can contribute to premature repolarization, loss of the dome and short APD. In the 25 patients studied here, short ARIs were never observed.

Supplementary Material

Refer to Web version on PubMed Central for supplementary material.

Acknowledgments

We greatly appreciate the able help and advice of Mr. Eric Novak with the statistical analysis. We also thank Ms. Julia Meyer for her assistance with recruiting the RBBB patients.

Funding Sources: This study was supported by NIH–National Heart, Lung, and Blood Institute grants R01-HL-033343 and R01-HL-049054 (to Y. Rudy) and by Washington University Institute of Clinical and Translational Sciences grant UL1-TR000448 from the National Center for Advancing Translational Sciences of the NIH. Y. Rudy is the Fred Saigh Distinguished Professor at Washington University.

References

1. Antzelevitch C, Brugada P, Borggrefe M, Brugada J, Brugada R, Corrado D, Gussak I, LeMarec H, Nademanee K, Riera ARP, Shimizu W, Schulze-Bahr E, Tan HL, Wilde AA. Brugada syndrome: Report of the second consensus conference endorsed by the Heart Rhythm Society and the European Heart Rhythm Association. Circulation. 2005; 111:659–670. [PubMed: 15655131]

2. Brugada P, Brugada J. Right bundle branch block, persistent ST segment elevation and sudden cardiac death: A distinct clinical and electrocardiographic syndrome. A multicenter report. J Am Coll Cardiol. 1992; 20:1391–1396. [PubMed: 1309182]

3. Antzelevitch C. Cellular basis and mechanism underlying normal and abnormal myocardial repolarization and arrhythmogenesis. Ann Med. 2004; 36:5–14. [PubMed: 15176418]

4. Szél T, Antzelevitch C. Abnormal repolarization as the basis for late potentials and fractionated electrograms recorded from epicardium in experimental models of Brugada syndrome. J Am Coll Cardiol. 2014; 63:2037–2045. [PubMed: 24657694]

5. Aiba T, Shimizu W, Hidaka I, Uemura K, Noda T, Zheng C, Kamiya A, Inagaki M, Sugimachi M, Sunagawa K. Cellular Basis for Trigger and Maintenance of Ventricular Fibrillation in the Brugada Syndrome ModelHigh-Resolution Optical Mapping Study. J Am Coll Cardiol. 2006; 47:2074–2085. [PubMed: 16697328]

6. Nademanee K, Veerakul G, Chandanamattha P, Chaothawee L, Ariyachaipanich A, Jirasirirojanakorn K, Likittanasombat K, Bhuripanyo K, Ngarmukos T. Prevention of ventricular fibrillation episodes in Brugada syndrome by catheter ablation over the anterior right ventricular outflow tract epicardium. Circulation. 2011; 123:1270–1279. [PubMed: 21403098]

7. Frustaci A, Priori SG, Pieroni M, Chimenti C, Napolitano C, Rivolta I, Sanna T, Bellocci F, Russo MA. Cardiac histological substrate in patients with clinical phenotype of Brugada syndrome. Circulation. 2005; 112:3680–3687. [PubMed: 16344400]

8. Tukkie R, Sogaard P, Vleugels J, de Groot IK, Wilde AA, Tan HL. Delay in right ventricular activation contributes to Brugada syndrome. Circulation. 2004; 109:1272–1277. [PubMed: 14993143]

9. Burnes JE, Taccardi B, MacLeod RS, Rudy Y. Noninvasive ECG imaging of electrophysiologically abnormal substrates in infarcted hearts: A model study. Circulation. 2000; 101:533–540. [PubMed: 10662751]

10. Ghanem RN, Burnes JE, Waldo AL, Rudy Y. Imaging dispersion of myocardial repolarization, II: Noninvasive reconstruction of epicardial measures. Circulation. 2001; 104:1306–1312. [PubMed: 11551884]

11. Ramanathan C, Ghanem RN, Jia P, Ryu K, Rudy Y. Noninvasive electrocardiographic imaging for cardiac electrophysiology and arrhythmia. Nat Med. 2004; 10:422–428. [PubMed: 15034569]

12. Ramanathan C, Jia P, Ghanem R, Ryu K, Rudy Y. Activation and repolarization of the normal human heart under complete physiological conditions. Proc Nat Acad Sci. 2006; 103:6309–6314. [PubMed: 16606830]

13. Cuculich PS, Zhang J, Wang Y, Desouza KA, Vijayakumar R, Woodard PK, Rudy Y. The electrophysiological cardiac ventricular substrate in patients after myocardial infarction: Noninvasive characterization with electrocardiographic imaging. J Am Coll Cardiol. 2011; 58:1893–1902. [PubMed: 22018301]

14. Rudy Y. Noninvasive electrocardiographic imaging of arrhythmogenic substrates in humans. Circ Res. 2013; 112:863–874. [PubMed: 23449548]

15. Vijayakumar R, Silva JNA, Desouza KA, Abraham RL, Strom M, Sacher F, Van Hare GF, Haïssaguerre M, Roden DM, Rudy Y. Electrophysiologic Substrate in Congenital Long QT Syndrome: Noninvasive Mapping with Electrocardiographic Imaging (ECGI). Circulation. 2014; 130:1936–1943. [PubMed: 25294783]

16. Coronel R, de Bakker JM, Wilms-Schopman FJ, Opthof T, Linnenbank AC, Belterman CN, Janse MJ. Monophasic action potentials and activation recovery intervals as measures of ventricular action potential duration: Experimental evidence to resolve some controversies. Heart Rhythm. 2006; 3:1043–1050. [PubMed: 16945799]

17. O'Hara T, Virág L, Varró A, Rudy Y. Simulation of the undiseased human cardiac ventricular action potential: Model formulation and experimental validation. PLoS Comput Biol. 2011; 7:e1002061. [PubMed: 21637795]

18. Clancy CE, Rudy Y. Na+ channel mutation that causes both Brugada and Long-QT syndrome phenotypes: A simulation study of mechanism. Circulation. 2002; 105:1208–1213. [PubMed: 11889015]

19. Durrer D, Van Dam RT, Freud G, Janse M, Meijler F, Arzbaecher R. Total excitation of the isolated human heart. Circulation. 1970; 41:899–912. [PubMed: 5482907]
20. Postema PG, van Dessel PF, de Bakker JM, Dekker LR, Linnenbank AC, Hoogendijk MG, Coronel R, Tijssen JG, Wilde AA, Tan HL. Slow and discontinuous conduction conspire in Brugada syndrome: A right ventricular mapping and stimulation study. Circ Arrhythm Electrophysiol. 2008; 1:379–386. [PubMed: 19808433]
21. Yokokawa M, Takaki H, Noda T, Satomi K, Suyama K, Kurita T, Kamakura S, Shimizu W. Spatial distribution of repolarization and depolarization abnormalities evaluated by body surface potential mapping in patients with Brugada syndrome. Pacing Clin Electrophysiol. 2006; 29:1112–1121. [PubMed: 17038144]
22. Coronel R, Casini S, Koopmann TT, Wilms-Schopman FJ, Verkerk AO, de Groot JR, Bhuiyan Z, Bezzina CR, Veldkamp MW, Linnenbank AC, van der Wal AC, Tan HL, Brugada P, Wilde AA, de Bakker JM. Right ventricular fibrosis and conduction delay in a patient with clinical signs of Brugada syndrome: A combined electrophysiological, genetic, histopathologic, and computational study. Circulation. 2005; 112:2769–2777. [PubMed: 16267250]
23. Kléber AG, Rudy Y. Basic mechanisms of cardiac impulse propagation and associated arrhythmias. Physiol Rev. 2004; 84:431–488. [PubMed: 15044680]
24. Wit AL, Josephson ME. Fractionated electrograms and continuous electrical activity: Fact or artifact. Card Electrophysiol Arrhyth. 1985:343–351.
25. Bébarová M, O'Hara T, Geelen JL, Jongbloed RJ, Timmermans C, Arens YH, Rodriguez L-M, Rudy Y, Volders PG. Subepicardial phase 0 block and discontinuous transmural conduction underlie right precordial ST-segment elevation by a SCN5A loss-of-function mutation. Am J Physiol Heart Circ Physiol. 2008; 295:H48–H58. [PubMed: 18456723]
26. Nagase S, Kusano KF, Morita H, Nishii N, Banba K, Watanabe A, Hiramatsu S, Nakamura K, Sakuragi S, Ohe T. Longer repolarization in the epicardium at the right ventricular outflow tract causes type 1 electrocardiogram in patients with Brugada syndrome. J Am Coll Cardiol. 2008; 51:1154–1161. [PubMed: 18355652]
27. Tokioka K, Kusano K, Morita H, Miura D, Nishii N, Nagase S, Nakamura K, Kohno K, Ito H, Ohe T. Electrocardiographic parameters and fatal arrhythmic events in patients with Brugada syndrome: Combination of depolarization and repolarization abnormalities. J Am Coll Cardiol. 2014; 63:2131–2138. [PubMed: 24703917]
28. Lambiase P, Ahmed A, Ciaccio E, Brugada R, Lizotte E, Chaubey S, Ben-Simon R, Chow A, Lowe M, McKenna W. High-density substrate mapping in Brugada syndrome: Combined role of conduction and repolarization heterogeneities in arrhythmogenesis. Circulation. 2009; 120:106–117. [PubMed: 19564561]
29. Chiale PA, Garro HA, Fernández PA, Elizari MV. High-degree right bundle branch block obscuring the diagnosis of Brugada electrocardiographic pattern. Heart Rhythm. 2012; 9:974–976. [PubMed: 22306100]
30. Giudicessi JR, Ye D, Tester DJ, Crotti L, Mugione A, Nesterenko VV, Albertson RM, Antzelevitch C, Schwartz PJ, Ackerman MJ. Transient outward current (Ito) gain-of-function mutations in the KCND3-encoded Kv4.3 potassium channel and Brugada syndrome. Heart Rhythm. 2011; 8:1024–1032. [PubMed: 21349352]

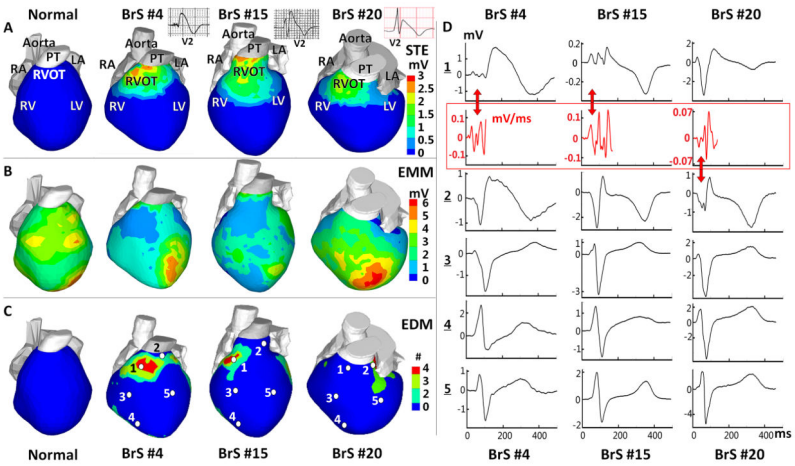

Figure 1.

Abnormal Epicardial Electrograms (EGMs) Characteristics and Localization. (A) Peak ST Segment elevation (STE) magnitude map. Insets show ECG lead V2. (B) EGM magnitude map (EMM). (C) EGM deflection map (EDM) showing number (#) of low amplitude deflections. BrS maps are in 3 right columns; left column shows corresponding maps from a normal subject for reference. (D) Unipolar EGMs from locations marked by white dots in Panel C. 1-Anterior RVOT, 2-Lateral RVOT, 3-RV free wall, 4-RV apex, 5-LV free wall (EGMs from other LV sites are also normal). Red traces: time derivatives of fractionated QRS. The derivatives approximate bipolar EGMs and emphasize fractionation. Maps are shown in anterior view. Each BrS column shows maps/EGMs from one patient identified by BrS#. RA: right atrium, LA: left atrium, RV: right ventricle, LV: left ventricle, RVOT: right ventricular outflow tract, PT: pulmonary trunk. Red arrows point to low voltage and fractionated EGMs.

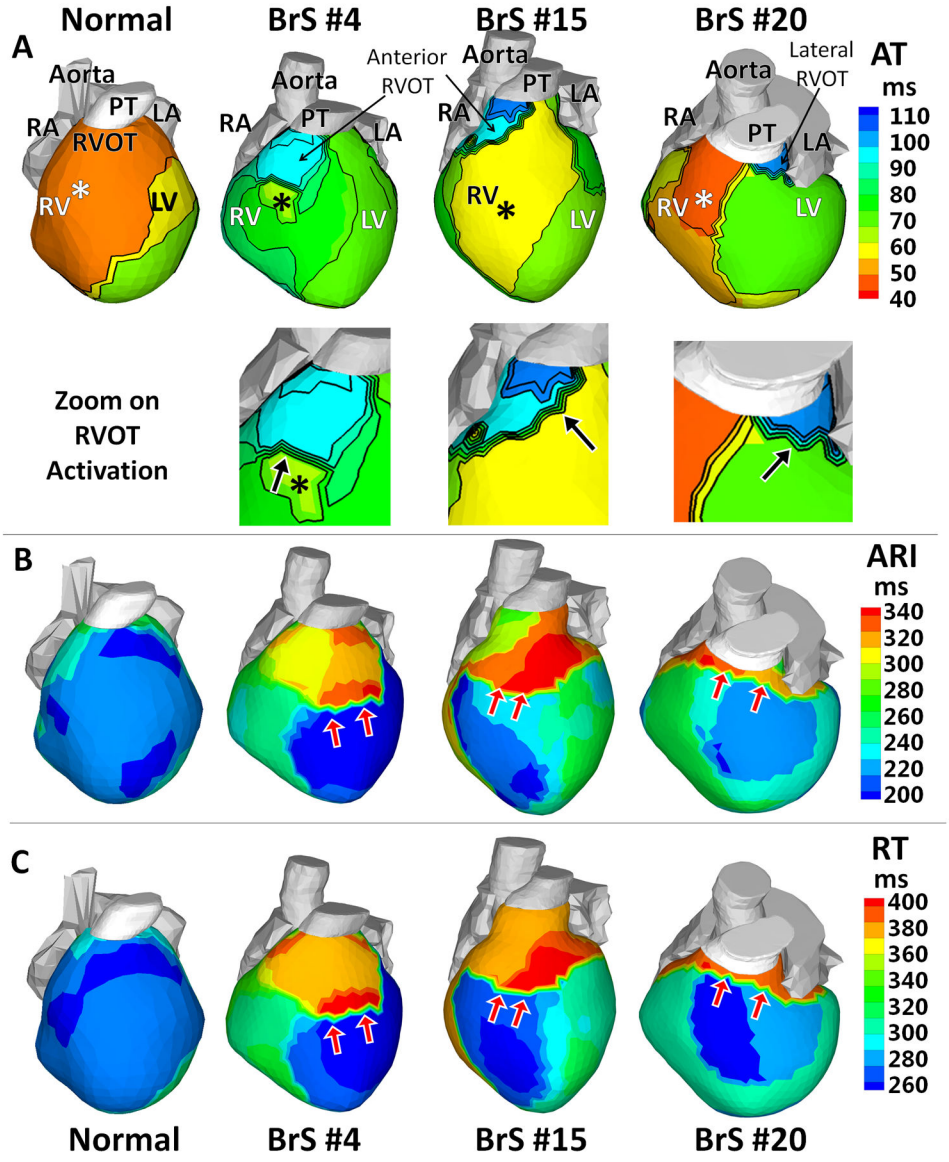

Figure 2.

Activation and Repolarization during Sinus Rhythm. (A) Activation times isochrone maps (AT). Lower panels: zoom on the RVOT. (B) Activation-recovery interval maps (ARI). (C) Recovery time maps (RT). Epicardial breakthroughs are indicated by asterisks. Isochrones are depicted in thin black lines. Black arrows in the RVOT zoom maps of Panel A point to slow conduction indicated by crowded isochronal lines. Red arrows in Panels B–C point to regions with steep repolarization gradients.

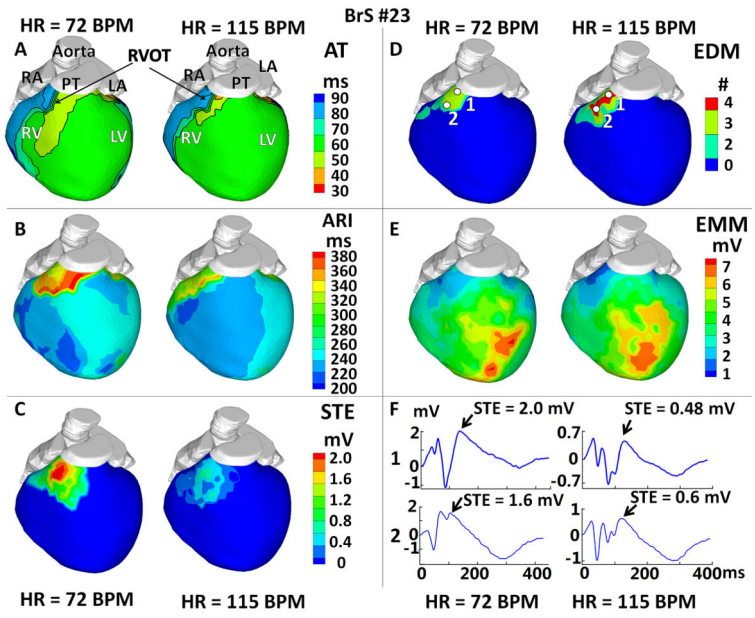

Figure 3.

Effects of Increased Heart Rate (HR). (A) Activation isochrone maps (AT). (B) Activation-recovery interval maps (ARI). (C) Peak ST segment elevation magnitude maps (STE). (D) Electrogram deflection maps (EDM), showing number (#) of deflection on EGM. (E) Electrogram magnitude maps (EMM). (F) EGMs from RVOT locations marked by white dots in Panel D. Each panel shows the map at resting (75 BPM) and increased HR (115 BPM).

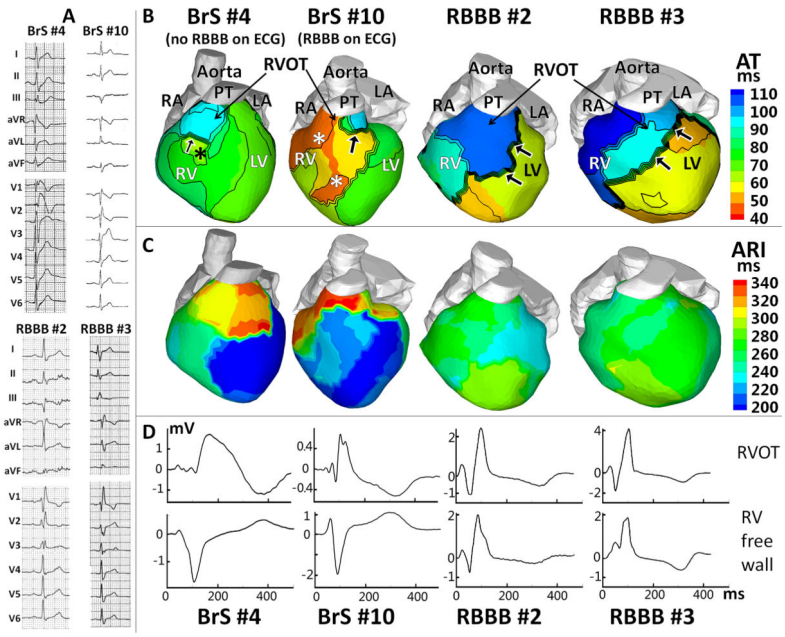

Figure 4.

Comparison between BrS and Non-BrS RBBB. (A) 12-lead ECGs. (B) Activation isochrone maps (AT). (C) Activation-recovery interval maps (ARI). (D) EGMs from the RVOT (top) and RV free wall (bottom). ECGs, maps and EGMs are shown for 4 representative examples (BrS#4: spontaneous Brugada ECG pattern. BrS#10: BrS patient with RBBB ECG pattern. RBBB#2 and RBBB#3: Non-BrS patients with RBBB ECG patterns). Epicardial breakthroughs are indicated by asterisks. Black arrows point to slow conduction in RVOT (BrS) or across the septum (RBBB).

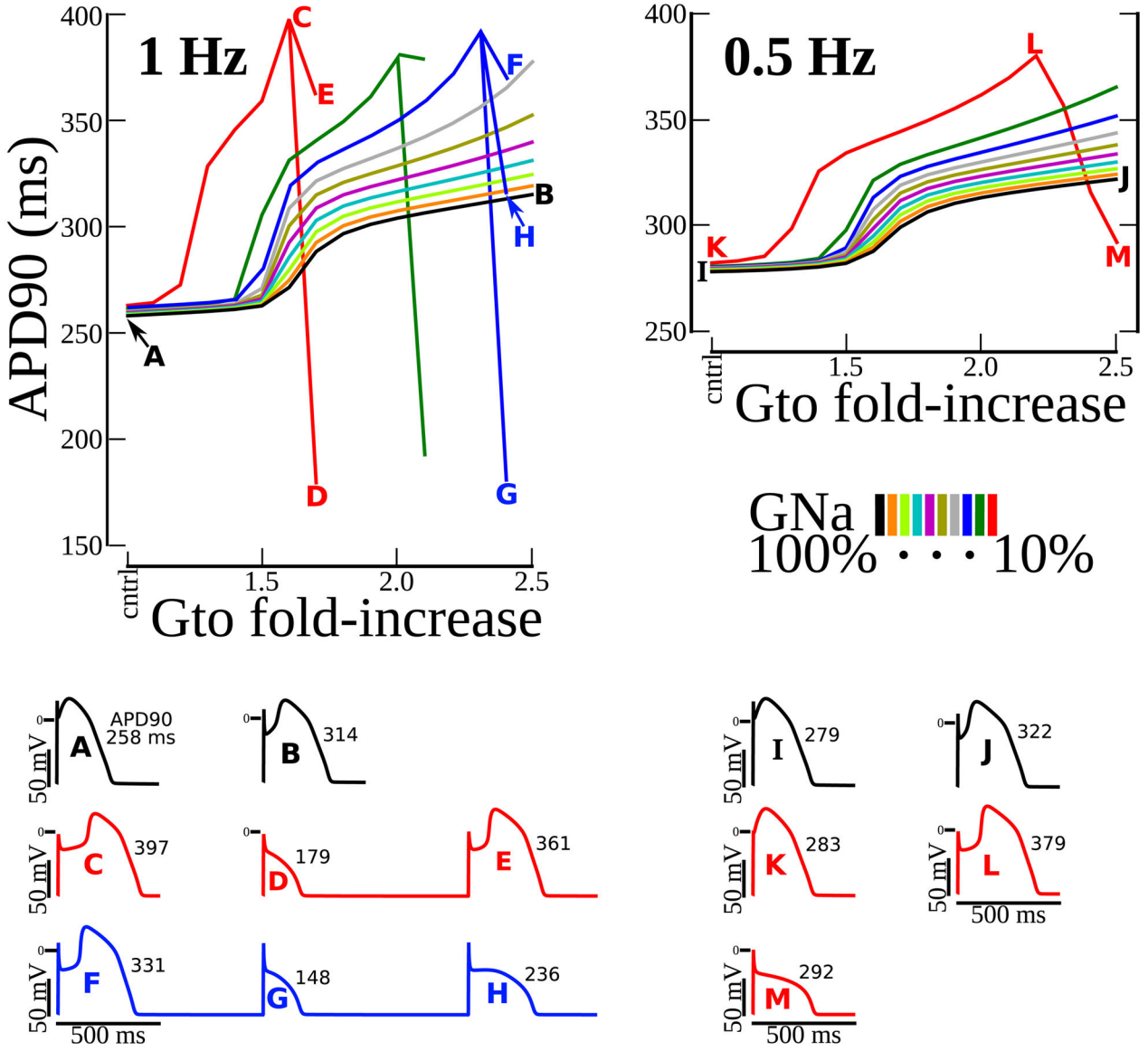

Figure 5.

Computer Simulation of BrS Effects on a Human RVOT AP. At pacing rate of 1 Hz and 0.5 Hz, APD90 (APD at 90% repolarization) was plotted versus I_{to} conductance increase (G_{to} from 1.0 to 2.5 fold). Colors indicate different amounts of I_{Na} conductance reduction (G_{Na} from 100 to 10%). APs and their duration are shown for G_{to}/G_{Na} pairings selected to illustrate the behaviors of interest: control– A and I; AP prolongation – B, C, E, F, J, and L; premature repolarization and AP shortening – D, G, H, and M; alternating AP prolongation and shortening – D, E, and F, G, H. Letters A through M relate the summary data above with each of the APs in the traces below. The simulations demonstrate bi-phasic changes of APD (prolongation followed by shortening). Prolongation was greater when I_{Na} was reduced. With I_{Na} loss, there was a critical degree of I_{to} enhancement beyond which APs fully

repolarized prematurely at phase-1, causing loss of plateau and APD shortening. Just below this critical degree, APs could alternate between premature repolarization and prolongation.

Table 1

ECGI Derived Parameters for BrS Patients

A. EGM Properties

B. Activation and Repolarization Parameters

C. Effects of Increased HR

D. Normal Values in RVOT

			RVOT	RV Free Wall	RV Apex	LV Base	LV Free Wall	LV Apex
A	Mean Peak STE (mV)		2.21±0.67	0.13±0.09*	0*	0*	0.08±0.04*	0*
	Mean EGM Magnitude (mV)		0.47±0.16 (Fractionated)	2.52±0.94*	3.77±0.85*	2.99±1.17*	3.14±0.81*	5.88±1.18*
	Mean EGM Fractionation (# of deflections)		2.97±0.69	1.04±0.80*	0*	0*	0*	0*
B	Mean AT (ms)		82±18	52±12*	57±7*	80±16	62±8*	58±10*
	Mean RT (ms)		381±30	272±42*	263±30*	317±38*	279±31*	272±31*
	Mean ARI (ms)		318±32	229±36*	221±37*	245±40*	222±31*	220±27*
C	Mean AT (ms)	Baseline HR	84±14	57±16	61±8	84±11	65±10	60±7
		Faster HR	81±19	56±15	63±7	84±10	63±8	58±8
	Mean RT (ms)	Baseline HR	392±26	265±38	274±34	333±42	284±39	281±38
		Faster HR	358±30§	251±35	265±29	320±36	275±33	274±37
	Mean ARI (ms)	Baseline HR	328±35	222±41	224±42	256±44	229±37	231±24
		Faster HR	287±33§	203±32	210±39	239±40	218±36	220±22
	Mean Peak STE (mV)	Baseline HR	2.56±0.71	0.09±0.08	0	0	0.13±0.04	0
		Faster HR	0.84±0.26§§	0.06±0.06	0	0	0.12±0.04	0
	Mean EGM Fractionation	Baseline HR	2.73±0.53	0.87±0.54	0	0	0	0
		Faster HR	3.65±0.60§§	1.09±0.41	0	0	0	0
D	Normal Values in RVOT		Peak STE=0 mV†	EGM Magnitude=3.74±1.60 mV†	EGM Fractionation=0†	AT=37±11 ms†	RT=311±34 ms†	ARI=241±27 ms†

Variables presented as mean±SD

*P<0.005 when comparing other segments to RVOT;

†P<0.005 when comparing variables in RVOT between normal control and BrS patients;

§ $p<0.05$ when compared to baseline HR;

§§ $p<0.005$ when compared to baseline HR.

EGM=Electrogram; HR=Heart Rate; AT=Activation Time; RT=Recovery Time; ARI= Activation-Recovery Interval.